Luminescent Platinum(II) Complexes. Electronic Spectroscopy of Platinum(II) Complexes of 2,2':6',2"-Terpyridine (terpy) and *p*-Substituted Phenylterpyridines and Crystal Structure of [Pt(terpy)Cl][CF_3SO_3]†

Hon-Kay Yip, Luk-Ki Cheng, Kung-Kai Cheung and Chi-Ming Che*
Department of Chemistry, The University of Hong Kong, Pokfulam Road, Hong Kong

The complexes $[Pt(terpy)L']^{n+}$ (terpy = 2,2':6',2"-terpyridine; L' = Cl, Br, I, N_3 or SCN^-, n = 1; L' = NH_3, n = 2) have been prepared and their spectroscopic and emission properties studied. Absorption bands are found at 300–350 and at 370–450 nm, which are assigned to the intraligand and metal-to-ligand charge-transfer (m.l.c.t.) transitions, respectively. The complexes [Pt(4'R-terpy)Cl]ClO_4 (R' = C_6H_4OMe-*p*, C_6H_4Me-*p*, C_6H_4Br-*p* or C_6H_4CN-*p*) were prepared by the reaction of $K_2[PtCl_4]$ with 4'R-terpy in water–MeCN. Unlike $[Pt(terpy)L']^{n+}$ which show emission in the solid state only, $[Pt(4'R\text{-}terpy)Cl]^+$ display ^{3}m.l.c.t. emission in fluid solution at room temperature. The crystal structure of [Pt(terpy)Cl][CF_3SO_3] has been determined: monoclinic, space group $P2_1/n$, a = 13.808(4), b = 6.873(1), c = 19.477(5) Å, β = 105.54(2)°, and Z = 4. In the unit cell, two $[Pt(terpy)Cl]^+$ cations stack in a head-to-tail fashion with an intermolecular Pt···Pt distance of 3.329(1) Å. The solid-state emission of [Pt(terpy)Cl][CF_3SO_3] is similar to that of the $^3(d_{\sigma^*}\pi^b)$ emission of the dinuclear complex $[Pt_2(terpy)_2L][ClO_4]_3$ (L = guadinate) having intramolecular Pt···Pt separations of 3.090(1) and 3.071(1) Å.

Luminescent platinum(II) complexes such as Pt(α-diimine)X_2 (X = halide or cyanide) and $[Pt(\alpha\text{-diimine})_2]^{2+}$ have been of much interest recently because they were found to display intriguing spectroscopic and photophysical properties.[1] Quite different from the octahedral complexes $[M(bipy)_3]^{n+}$ (M = d^6 metal ion, bipy = 2,2'-bipyridine), some of these platinum(II) complexes were found to exhibit solid-state excimeric emission, which is an interesting phenomena in co-ordination chemistry.[1a,c,d] In their study on the solid-state photoluminescence of $[Pt(bipy)X_2]^{n+}$ and $[Pt(phen)X_2]^{n+}$ (phen = 1,10-phenanthroline; X = halide, n = 0; X = ½ bipy or phen, n = 2), Miskowski and Houlding[1a] suggested that the platinum(II) excited state interacts with its ground state *via* π–π interaction of the α-diimine ligands.[1a] The red form of $[Pt(bipy)(CN)_2]$ the solid-state emission of which is of considerably low energy and structureless, has been shown to stack in a head-to-head fashion.[1e] Its solid-state emission along with those of other stacking $[Pt(\alpha\text{-diimine})(CN)_2]$ complexes were suggested to arise from a $^3(d_{\sigma^*}\pi^b)$ excited state, where the π^b and d_{σ^*} orbitals are formed from the bonding interaction of the π^* orbitals of the α-diimines and the antibonding interaction of the platinum(II) $5d_{z^2}$ orbitals, respectively.[1b] A molecular orbital diagram[1b] describing such interaction is shown in Fig. 1.

The solution photochemistry of this class of complexes is also intriguing. The complexes [Pt(dpphen)$(CN)_2$] (dpphen = 4,7-diphenyl-1,10-phenanthroline)[1d] and [Pt(dbbipy)$(CN)_2$] (dbbipy = 4,4'-di-*tert*-butyl-2,2'-bipyridine)[1c] were reported to form emissive excimers at high concentrations. In order to understand the excimeric and solid-state interaction of the platinum(II) polypyridyl complexes, we investigated the spectroscopic and photophysical properties of a dinuclear model complex $[Pt_2(terpy)_2L]^{3+}$ [terpy = 2,2':6',2"-terpyridine; HL = guanidine, H_2N–C(=NH)–NH_2] the structure of which is shown in Fig. 2.[2] It is expected that a clear understanding of mononuclear $[Pt(terpy)L']^{n+}$ (L' = Cl, Br, I, N_3 or SCN^-, n = 1; L' = NH_3, n = 2) complexes is complementary to the study of $[Pt_2(terpy)_2L]^{3+}$.[2] Hence their spectroscopic properties were also investigated. The crystal structure of [Pt(terpy)Cl][CF_3SO_3] has been determined and its solid-state spectroscopic properties are compared with those of $[Pt_2(terpy)_2L]^{3+}$.

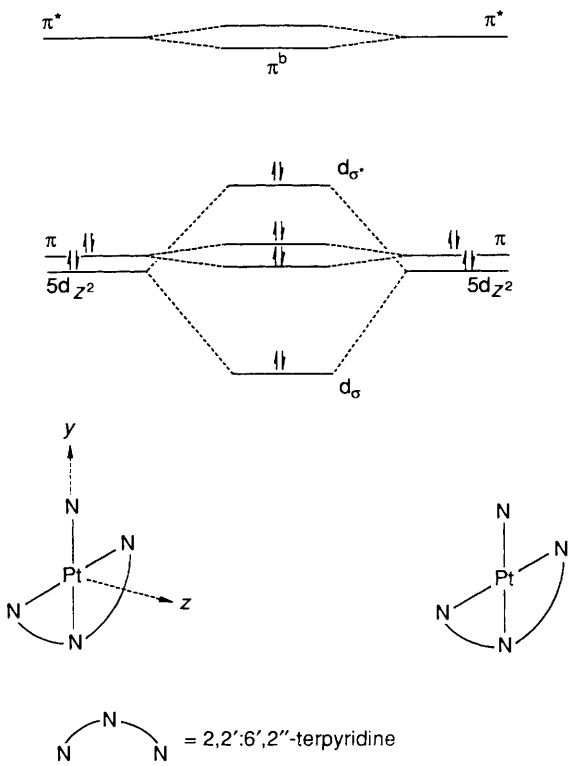

Fig. 1 A molecular orbital diagram describing the Pt···Pt and ligand–ligand interactions in $[Pt_2(terpy)_2L]^{3+}$

† *Supplementary data available:* see Instructions for Authors, *J. Chem. Soc., Dalton Trans.*, 1993, Issue 1, pp. xxiii–xxviii.

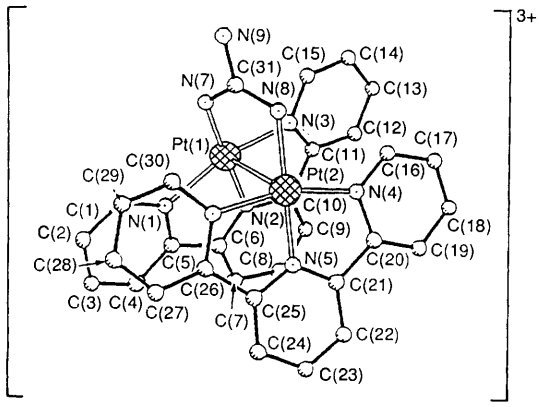

Fig. 2 The structure of $[Pt_2(terpy)_2L]^{3+}$

Experimental

Materials.—Potassium tetrachloroplatinate (>99.99%), 2,2′:6′,2″-terpyridine (terpy) (98%) and guanidine carbonate $2NH_2$–C(=NH)–NH_2·H_2CO_3 (99%) were obtained from Aldrich. Acetonitrile for spectroscopic and emission lifetime measurements was purified by distillation over $KMnO_4$. The complex $[Pt_2(terpy)_2L][ClO_4]_3$[2] and the ligands 4′-(*p*-methoxyphenyl)-2,2′:6′,2″-terpyridine (mpterpy), 4′-tolyl-2,2′:6′,2″-terpyridine (tterpy), 4′-(*p*-bromophenyl)-2,2′:6′,2″-terpyridine (bpterpy) and 4′-(*p*-cyanophenyl)-2,2′:6′,2″-terpyridine (cpterpy) were prepared by literature methods.[3]

Preparations.—[Pt(terpy)Cl][CF_3SO_3]. An aqueous solution (30 cm^3) of AgO_3SCF_3 (0.15 g, 0.60 mmol) and [Pt(terpy)Cl]Cl[4] (0.3 g, 0.60 mmol) was refluxed for 0.5 h. This was then filtered to remove the insoluble AgCl and the filtrate evaporated to give a yellow solid, which was extracted with acetonitrile. To the acetonitrile extract was added diethyl ether. An orange precipitate was obtained. The compound was recrystallized by diffusing diethyl ether into an acetonitrile solution (yield = 63%) (Found: C, 31.1; H, 2.0; N, 6.70. Calc. for $C_{16}H_{11}ClF_3N_3O_3PtS$: C, 31.3; H, 1.80; N, 6.85%).

[Pt(terpy)L′]PF_6 (L′ = Br, I *or* SCN). To an aqueous solution (30 cm^3) of [Pt(terpy)Cl]Cl (0.20 g) was added an excess of NaX (0.5 g) (X = Br, I or SCN). A deep orange precipitate was obtained immediately. The solid was dissolved in water (≈ 50 cm^3) and NH_4PF_6 was added to give a yellow (X = Br or I) or red (X = SCN) precipitate. The crude product was recrystallized by diffusion of diethyl ether into an acetonitrile solution (yields for X = Br, I and SCN were 40, 36 and 68%, respectively) (Found: C, 27.8; H, 1.7; N, 6.3. Calc. for $C_{15}H_{11}BrF_6N_3PPt$: C, 27.6; H, 1.7; N, 6.4. Found: C, 25.4; H, 1.5; N, 5.5. Calc. for $C_{15}H_{11}F_6IN_3PPt$: C, 25.7; H, 1.6; N, 6.0. Found: C, 30.6; H, 1.5; N, 9.0. Calc. for $C_{16}H_{11}F_6N_4PPt$: C, 30.4; H, 1.7; N, 8.9%). Infrared data for [Pt(terpy)(SCN)]PF_6: 2100s (sh), ν(C≡N); 1602m (sh), ν(C–C) of terpy; 842s (br) cm^{-1}, ν(PF_6^-).

[Pt(terpy)L′][PF_6]$_z$ (L′ = NH_3, z = 2; L′ = N_3^-, z = 1). To an aqueous solution of [Pt(terpy)Cl]Cl was added an excess of 35% ammonia solution (L′ = NH_3) or sodium azide (L′ = N_3^-). A clear deep yellow solution was immediately obtained which was filtered. Upon addition of NH_4PF_6 a yellow solid was obtained, which was recrystallized by diffusion of diethyl ether into an acetonitrile solution. The colour of [Pt(terpy)-(NH_3)][PF_6]$_2$ was red but became dull yellow after standing in air for 1 d. The colour of [Pt(terpy)(N_3)]PF_6 remained red for days (yields were 69 and 75%, respectively) (Found: C, 24.3; H, 1.7; N, 7.4. Calc. for $C_{15}H_{14}F_{12}N_4P_2Pt$: C, 24.5; H, 1.9; N, 7.6. Found: C, 29.0; H, 1.7; N, 13.4. Calc. for $C_{15}H_{11}F_6N_6PPt$: C, 29.3; H, 1.8; N, 13.7%). ^{1}H NMR for [Pt(terpy)(NH_3)][PF_6]$_2$: δ 2.57 (s, 3 H, NH_3), 7.6–8.8 (m, 11 H, terpy). Infrared data for [Pt(terpy)(N_3)]PF_6: 2064s (sh), ν(N≡N); 1605m (sh), ν(C–C) of terpy; 840 s (sh) cm^{-1}, ν(PF_6^-).

[Pt(4′R-terpy)Cl]ClO_4 (R = C_6H_4OMe-*p*, C_6H_4Me-*p*, C_6H_4Br-*p* *or* C_6H_4CN-*p*). A mixture of 4R′-terpy (0.25 mmol) and $K_2[PtCl_4]$ (0.25 mmol) in water–MeCN (1 : 1 v/v, 30 cm^3) was refluxed for 24 h. The resulting suspension was filtered while hot into a solution of $NaClO_4$ (0.5 g) in water (10 cm^3). The precipitate was filtered off, washed with water and ethanol and recrystallized by diffusing diethyl ether into a MeCN–$HCONMe_2$ solution.

[Pt(mpterpy)Cl]ClO_4 (Found: C, 40.3; H, 2.2; N, 6.5. Calc. for $C_{22}H_{17}Cl_2N_3O_5Pt$: C, 40.4; H, 2.6; N, 6.4%), ^{1}H NMR δ 3.93 (s, 3 H), 7.19 (d, 2 H), 7.79 (d, 2 H), 7.98 (d, 2 H), 8.35 (m, 4 H), 8.38 (s, 2 H) and 8.97 (d, 2 H). [Pt(tterpy)Cl]ClO_4 (Found: C, 41.2; H, 2.9; N, 7.1. Calc. for $C_{22}H_{17}Cl_2N_3O_4Pt$: C, 40.4; H, 2.6; N, 6.4%), ^{1}H NMR δ 2.47 (s, 3 H), 7.48 (d, 2 H), 7.80 (t, 2 H), 7.90 (d, 2 H), 8.36 (m, 4 H), 8.44, (s, 2 H) and 8.98 (d, 2 H). [Pt(bpterpy)Cl]ClO_4 (Found: C, 34.8; H, 1.7; N, 5.9. Calc. for $C_{21}H_{14}BrCl_2N_3O_4Pt$: C, 35.1; H, 2.0; N, 5.9%): ^{1}H NMR δ 7.92 (d, 2 H), 7.96 (dd, 2 H), 8.16 (d, 2 H), 8.55 (dd, 2 H), 8.83, (d, 2 H), 8.93 (d, 2 H) and 8.99 (s, 2 H). [Pt(cpterpy)Cl]ClO_4 (Found: C, 38.8; H, 2.3; N, 8.0. Calc. for $C_{22}H_{14}Cl_2N_4O_4Pt$: C, 39.8; H, 2.1; N, 8.4%): IR 2226s (sh) cm^{-1}, ν(C≡N); ^{1}H NMR δ 7.82 (td, 2 H), 8.03 (d, 2 H), 8.10 (d, 2 H), 8.36 (m, 4 H), 8.46 (s, 2 H) and 8.98 (d, 2 H).

Instrumentation.—The UV/VIS absorption spectra were recorded on a Milton Roy Spectronic 3000 diode-array spectrophotometer, emission spectra on a Spex Fluorolog-2 spectrofluorometer, infrared spectra as Nujol mulls on a Nicolet 20SX FT–IR spectrometer and ^{1}H NMR spectra (in CD_3CN) on a JEOL GSX 270 MHz spectrometer with $SiMe_4$ as standard. Emission lifetimes and transient absorption spectra were studied with the laser photolysis set-up described elsewhere.[1c] Solution emission quantum yields were measured with a degassed acetonitrile solution of [Ru(bipy)$_3$][ClO_4]$_2$ as reference.

Crystal Structure Determination.—*Crystal data.* $C_{16}H_{11}ClF_3N_3O_3PtS$, M = 612.89, monoclinic, space group $P2_1/n$, a = 13.808(4), b = 6.873(1), c = 19.477(5) Å, β = 105.54(2)°, U = 1780.9(1.0) Å^3, Z = 4, D_c = 2.286 g cm^{-3}, μ(Mo-Kα) = 82.8 cm^{-1}, F(000) = 1160.

A crystal of dimensions of 0.08 × 0.1 × 0.2 mm was used for data collection at 24 °C on a Enraf-Nonius CAD-4 diffractometer with graphite-monochromatized Mo-Kα radiation (λ = 0.710 73 Å) using ω–2θ scans with ω-scan angles (0.60 + 0.344 tan θ)° at speeds of 1.18–8.24° min^{-1}. Intensity data ($2\theta_{max}$ = 56°, h 0–18, k 0–9, l −25 to 25) were corrected for Lorentz and polarization effects and empirical absorption based on a ψ scan of three strong reflections. Upon averaging the 4902 reflections, 4652 independent ones were obtained and 2836 with $F_o \geqslant 3\sigma(F_o)$ were considered observed and used in the structural analysis. The space group was determined from systematic absences and the structure was solved by Patterson and Fourier methods and refined by full-matrix least squares using the Enraf-Nonius programs[5] on a MicroVAX II computer. All non-H atoms were refined anisotropically. Convergence for 253 variables by least-squares refinement with $w = 4F_o^2/\sigma^2(F_o^2)$ where $\sigma^2(F_o^2) = [\sigma^2(I) + (0.04F_o^2)^2]$ was reached at R = 0.028, R' = 0.034 and S = 1.033; $(\Delta/\sigma)_{max}$ = 0.01. A final Fourier difference map was featureless, with maximum positive and negative peaks of 0.58 and 0.62 e Å^{-3} respectively. Table 1 lists the atomic coordinates of the non-hydrogen atoms and selected bond distances and angles are given in Table 2.

Additional material available from the Cambridge Crystallographic Data Centre comprises H-atom coordinates, thermal parameters and remaining bond lengths and angles.

Results and Discussion

Previous studies of platinum(II) terpy complexes mainly focused on their interaction with biological molecules like

Table 1 Atomic coordinates of non-hydrogen atoms of [Pt(terpy)Cl][CF_3SO_3]

Atom	*x*	*y*	*z*
Pt	0.009 89(1)	0.259 00(3)	0.497 06(1)
Cl	−0.1194(1)	0.2476(2)	0.393 69(7)
S	0.0346(1)	0.4571(3)	0.168 87(9)
F(1)	−0.0528(5)	0.7912(7)	0.1309(3)
F(2)	0.0016(4)	0.6604(9)	0.0510(2)
F(3)	−0.1295(4)	0.5481(8)	0.0728(3)
O(1)	−0.0190(3)	0.4471(8)	0.2224(2)
O(2)	0.1294(3)	0.5547(9)	0.1904(3)
O(3)	0.0335(5)	0.2839(8)	0.1293(3)
N(1)	−0.0695(4)	0.1891(7)	0.5668(2)
N(2)	0.1176(3)	0.2634(6)	0.5838(2)
N(3)	0.1256(3)	0.3297(7)	0.4559(2)
C(1)	−0.1684(4)	0.1496(8)	0.5519(3)
C(2)	−0.2138(5)	0.1002(9)	0.6048(3)
C(3)	−0.1566(5)	0.091(1)	0.6733(4)
C(4)	−0.0541(5)	0.1314(9)	0.6902(3)
C(5)	−0.0112(5)	0.1821(8)	0.6358(3)
C(6)	0.0946(4)	0.2297(7)	0.6462(3)
C(7)	0.1701(5)	0.2380(8)	0.7088(3)
C(8)	0.2684(5)	0.2740(9)	0.7059(3)
C(9)	0.2894(5)	0.3102(9)	0.6418(3)
C(10)	0.2111(4)	0.3048(8)	0.5803(3)
C(11)	0.2161(4)	0.3415(8)	0.5061(3)
C(12)	0.3018(5)	0.3857(9)	0.4876(3)
C(13)	0.2975(5)	0.426(1)	0.4164(3)
C(14)	0.2064(5)	0.4121(9)	0.3663(3)
C(15)	0.1211(4)	0.3641(8)	0.3862(3)
C(16)	−0.0391(6)	0.621(1)	0.1027(4)

Table 2 Selected bond lengths (Å) and angles (°) of [Pt(terpy)Cl][CF_3SO_3]

Pt–Cl	2.307(1)	Pt–N(1)	2.018(5)
Pt–N(2)	1.930(4)	Pt–N(3)	2.030(5)
Cl–Pt–N(1)	98.5(1)	Cl–Pt–N(2)	178.9(1)
Cl–Pt–N(3)	99.8(1)	N(1)–Pt–N(2)	81.1(2)
N(1)–Pt–N(3)	161.8(2)	N(2)–Pt–N(3)	80.8(2)
N(2)–C(6)–C(5)	112.3(4)	N(2)–C(10)–C(11)	112.4(4)

DNA and metalloproteins, as highlighted by the works of Lippard[6] and Kostic[7] and co-workers. This work presents a study of the spectroscopic and luminescent properties of the complexes. Gray and co-workers[8] recently reported a similar study on the related $[Pt_2(terpy)_2L'']^{3+}$ complexes (L'' = pyrazolate, azaindolate, diphenylformamidinate or argininate) which have similar structure to that of $[Pt_2(terpy)_2L]^{3+}$ studied in this work.

Electronic Spectroscopy and Photophysics of [Pt(terpy)L']$^{n+}$ *and* [Pt(4'R-terpy)Cl]$^+$.—There have been few spectroscopic studies on platinum(II) terpy complexes. Lippard and co-workers[6] reported the electronic absorption spectra of [Pt(terpy)Cl]Cl and [Pt(terpy)(SCH_2CH_2OH)]NO_3 but no assignments were given. In this work several such complexes were prepared by ligand-substitution reactions of [Pt(terpy)Cl]$^+$. As representative examples of this class of complexes, the electronic absorption spectra of [Pt(terpy)Cl][CF_3SO_3], [Pt(terpy)I]PF_6, and [Pt(terpy)(NH_3)][PF_6]$_2$ in acetonitrile are shown in Fig. 3. The electronic spectral data for the other complexes are listed in Table 3. On the whole, all these complexes show broad absorption at 370–450 nm ($\varepsilon \approx 10^3$ dm^3 mol^{-1} cm^{-1}, band A) and an intense band with distinct vibronic structures at 300–350 nm ($\varepsilon > 10^4$ dm^3 mol^{-1}, band B).

Because band A is broad, it is difficult to locate its maximum. As there is no corresponding absorption band for $[Zn(terpy)_2]^{2+}$,[9] we tentatively assign it to the metal-to-ligand

Table 3 Spectroscopic data for [Pt(terpy)L']$^{n+}$*

	Band [λ/nm (10^{-4} ε_{max}/dm^3 mol^{-1} cm^{-1})]	
L'	A	B
Cl	372 (0.13), 398 (0.12)	304 (0.64), 317 (0.72), 333 (1.01), 345 (0.58)
Br	400 (0.14)	307 (0.74), 320 (0.80), 330 (1.07), 350 (0.59)
I	387 (0.33), 452 (0.75)	304 (1.06), 319 (1.15), 333 (1.33), 348 (1.06)
SCN	403 (0.22)	354 (0.93)
N_3	374 (0.19), 385 (0.09)	314 (0.61), 328 (0.700), 348 (0.96)
NH_3	373 (0.12), 391 (0.04)	328 (0.72), 343 (1.13)

* All data were obtained in acetonitrile solution at room temperature.

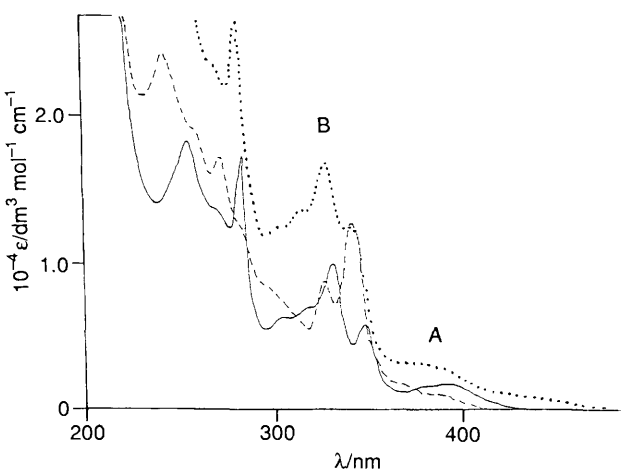

Fig. 3 The UV/VIS absorption spectra of [Pt(terpy)Cl][CF_3SO_3] (——), [Pt(terpy)(NH_3)][PF_6]$_2$ (– – –), and [Pt(terpy)I]PF_6 (• • •) in acetonitrile

charge-transfer (m.l.c.t) transition Pt(5d)→terpy (π*). In general, m.l.c.t. transitions of platinum(II) α-diimine complexes are rarely observed because they are usually obscured by the intraligand (i.l.) transition of the diimine ligands. Houlding and Miskowski[1f] reported that the m.l.c.t. transition of dichloro(3,3'-dicarboxy-2,2'-bipyridine)platinum occurs at 444 nm (ε = 3030 dm^3 mol^{-1} cm^{-1}), which is within the energy range of band A of [Pt(terpy)L']$^{n+}$ studied in this work, and the ε_{max} values of band A of [Pt(terpy)L']$^{n+}$ also compare favourably with that of the above band of the bipy complex.

The vibronically structured band B with vibrational spacings ranging from 1270 to 1395 cm^{-1} is suggested to be due to the $^1(\pi \longrightarrow \pi^*)$ transition of terpy. Interestingly the band profile depends on the nature of L' in [Pt(terpy)L']$^{n+}$. For L' = Cl, Br or I the absorption band strongly resembles the intraligand π–π* transition the ratios of the molar absorptivity *a*(348 nm)/*a*(333 nm) being >1:1. For [Pt(terpy)(NH_3)]$^{2+}$ and [Pt(terpy)(N_3)]$^+$, the corresponding ratios are <1:1. We rationalize this finding by the mixing between the i.l. and m.l.c.t. excited states of [Pt(terpy)L']$^{n+}$, the extent of which depends on the nature of ligand L'. Configuration interaction between m.l.c.t. and i.l. excited states was observed for d^6 α-diimine complexes before.[10,11] For example, in the case of $[Ir(dmphen)_2Cl_2]^+$(dmphen = 4,7-dimethyl-1,10-phenanthroline), these two excited states are close in energy and a change of solvent was found to alter the degree of mixing between them.[10] The interplay of m.l.c.t., i.l. and ligand-field excited states of $[Ru(bipy)_2(MeNC)_2]^+$, $[Ru(bipy)_2(CN)(MeNC)]^+$ and $[Ru(bipy)(MeNC)_4]^{2+}$ was also found to be controlled by the auxiliary ligands.[11] Here, [Pt(terpy)L']$^{n+}$ are co-

ordinatively unsaturated and resemble the co-ordinatively saturated complexes of Ir^{III} and Ru^{II} in this context.

All $[Pt(terpy)L']^{n+}$ are strongly emissive in solid form at room temperature. The solid-state emission lifetimes (measured at room temperature) of the yellow forms of $[Pt(terpy)(NH_3)][PF_6]$, $[Pt(terpy)Br]PF_6$ and $[Pt(terpy)I]PF_6$ are 0.5, 0.3 and 0.6 μs respectively while those of the red solid samples of $[Pt(terpy)Cl][CF_3SO_3]$, $[Pt(terpy)(SCN)]PF_6$ and $[Pt(terpy)(N_3)]PF_6$ are 0.2, 0.4 and 0.2 μs respectively. Fig. 4 shows the emission spectra of $[Pt(terpy)Cl]^+$ and $[Pt(terpy)(NH_3)]^{2+}$ measured in butyronitrile glass. The emission spectra of $[Pt(terpy)L']^+$ (L' = Cl, Br, I or N_3) are similar. They are all vibronically structured with spacings between the 0–0 and 0–1 transitions of ≈1420 cm^{-1}. The Huang–Rhys factors, defined as I_{0-1}/I_{0-0}, of $[Pt(terpy)L']^+$ (L' = halide or N_3) are all ≈0.6. We tentatively assign the emissions of these complexes to ^{3}m.l.c.t. [Pt→terpy(π*)].

Although the emission of $[Pt(terpy)(NH_3)]^{2+}$ is also vibronically structured, its spectral profile is different from that of $[Pt(terpy)L']^+$ as discussed above. Its spectrum is more complicated, consisting of more than one vibronic progression, and highly resembles that of the free ligand terpy.[12] From the emission profiles the emissive excited state of $[Pt(terpy)(NH_3)]^{2+}$ appears to have substantial intraligand (terpy) character while $[Pt(terpy)L']^+$ (L' = halide or N_3) have a 'm.l.c.t.-like' emissive state.

Although $[Pt(terpy)L']^{n+}$ are strongly luminescent materials in the solid state, no emission was observed in fluid solution at room temperature. This lack of emission is probably due to low-lying d–d excited states, which provide facile deactivation pathways *via* molecular distortion. The d–d and m.l.c.t. excited states of the platinum(II) terpy complexes may be very close in energy. Houlding and Miskowski[1f] estimated the energy of the 0–0 ligand-field transition of various Pt(α-diimine) complexes to be 18 000–19 500 cm^{-1} which is just lower in energy than the 0–0 m.l.c.t. transition of $[Pt(bipy)Cl_2]$ (estimated at about 20 408 cm^{-1}). We argue that the increase in energy difference between the ligand-field and m.l.c.t. excited states is a means of constructing long-lived and emissive platinum(II) polypyridyl complexes. Recently, McMillin and co-workers[13] reported that $[Ru(dpterpy)_2]^{2+}$ (dpterpy = 4,4'-diphenyl-2,2':6',2''-terpyridine) or $[Ru(tpterpy)]^{2+}$ (tpterpy = 4,4',4''-triphenyl-2,2':6',2''-terpyridine) have longer emission lifetimes and greater quantum yields than those of $[Ru(terpy)_2]^{2+}$. This was attributed to the low-lying π* orbital of the substituted terpy ligands, which leads to an increase in energy gap between the m.l.c.t. and ligand-field excited states. Thus it is reasonable to expect that platinum(II) complexes of 4R'-terpy may also possess a long-lived ^{3}m.l.c.t. state.

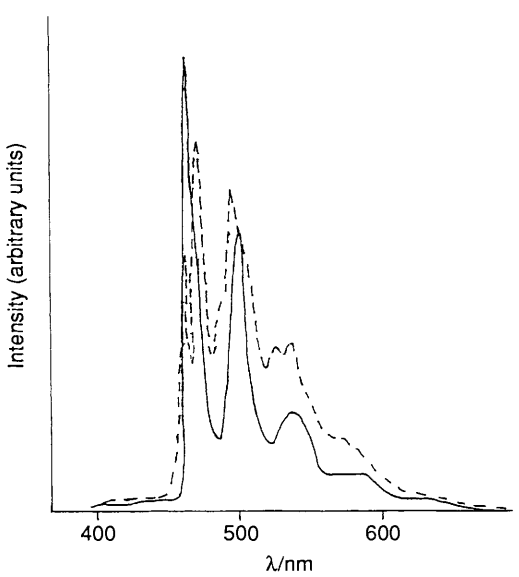

Fig. 4 Emission spectra of $[Pt(terpy)Cl][CF_3SO_3]$ (——) and $[Pt(terpy)(NH_3)][PF_6]_2$ (– – – –) in a butyronitrile glass at 77 K

In this work, $[Pt(4'R\text{-}terpy)Cl]^+$ complexes have been synthesised and characterized by spectroscopic means. Fig. 5 shows the UV/VIS absorption spectrum of $[Pt(mpterpy)Cl]ClO_4$ and the free ligand mpterpy. The spectrum of the complex exhibits intense absorption bands at 283 (1.18×10^4) and 337 nm ($\varepsilon = 6.69 \times 10^3$ dm^3 mol^{-1}), which are also present for mpterpy, assigned to the intraligand transitions. On the other hand, the moderately intense absorption band at 415 nm ($\varepsilon = 3.904 \times 10^3$ dm^3 mol^{-1} cm^{-1}), which is substantially red-shifted from the absorption spectrum of $[Pt(terpy)Cl]^+$, is tentatively assigned to the spin-allowed m.l.c.t. transition. The spectra of other $[Pt(4'R\text{-}terpy)Cl]ClO_4$ complexes are similar and their electronic spectral data are given in Table 4.

Unlike $[Pt(terpy)L']^{n+}$, all $[Pt(4'R\text{-}terpy)Cl]ClO_4$ display emission in degassed acetonitrile solution at room temperature. Photophysical data for the complexes are given in Table 4. Fig. 5 shows the emission spectrum of $[Pt(mpterpy)Cl]ClO_4$ measured in acetonitrile at room temperature. The excitation spectrum for the emission closely resembles the absorption spectrum. Since the emission of the free ligand mpterpy occurs at higher energy (emission maximum at ≈500 nm at 77 K), we tentatively assign the emission of $[Pt(mpterpy)Cl]^+$ as arising from a ^{3}m.l.c.t. excited state. To our knowledge, apart from some cyclometallated platinum(II) complexes,[14] there are few examples of platinum(II) polypyridyl complexes which exhibit ^{3}m.l.c.t. emission in fluid solution. The emission bands of all other $[Pt(4'R\text{-}terpy)Cl]^+$ are also structureless except that of R' = C_6H_4CN-*p*, which is vibronically structured with progression of about 1040 cm^{-1}.

Crystal Structure and Spectroscopic Properties of the Solid $[Pt(terpy)Cl][CF_3SO_3]$.—It is known that the colour of $[Pt(terpy)L']^{n+}$ varies from yellow to deep red, depending on the method of preparation and crystallization.[15] We have also found that an acetonitrile solution of $[Pt(terpy)Cl][CF_3SO_3]$

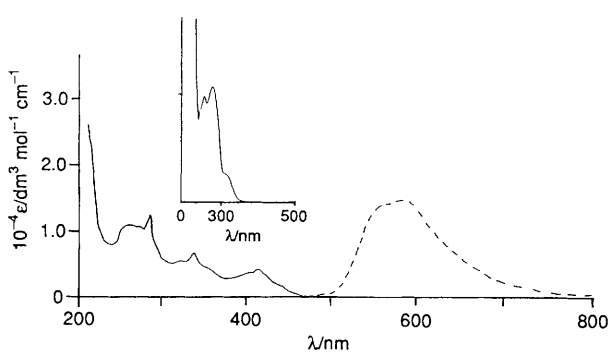

Fig. 5 Absorption (——) and emission (– – – –) spectra of $[Pt(mpterpy)Cl]ClO_4$ in acetonitrile at room temperature. Insert is the absorption spectrum of mpterpy in dichloromethane

Table 4 Spectroscopic and photophysical data for $[Pt(4'R\text{-}terpy)Cl]ClO_4$

	λ_{max}/cm^{-1} (ε/dm^3 mol^{-1} cm^{-1})			
R	*a*	*b*	τ^c/μs	$10^3\varphi^d$
C_6H_4OMe-*p*	24 100 (3904)	17 180	8.5	14
C_6H_4Me-*p*	24 510 (4343)	17 480	2.4	0.7
C_6H_4Br-*p*	24 690 (6177)	18 760	1.3	0.4
C_6H_4CN-*p*	24 750 (7910)	18 870	0.8	2.5

[a] Absorption maximum for the ^{1}m.l.c.t. transition. [b] Emission maximum. [c] Emission lifetime. [d] Quantum yield of emission.

is light yellow while the crystalline form of the complex is orange-red. Analogous behaviour has been observed for other Pt-(α-diimine) complexes.[1a,e] In order to rationalize this finding an X-ray analysis of solid $[Pt(terpy)Cl][CF_3SO_3]$ was undertaken.

Fig. 6 shows a perspective view of the $[Pt(terpy)Cl]^+$ cation. The co-ordination of Pt is slightly distorted square planar. In the unit cell two complex cations stack in a head-to-tail orientation with an intermolecular Pt···Pt separation of 3.329(1) Å. This distance is significantly shorter than values of 3.5721(8) and 3.45 Å for other head-to-tail stacking complexes $[Pt(terpy)(SCH_2CH_2OH)]NO_3$[6] and the red form of $[Pt(bipy)Cl_2]$,[16] and even comparable to the intramolecular Pt···Pt separation of 3.301(1) Å in $[Pt_2(dppm)_2(CN)_4]$ [dppm = bis(diphenylphosphino)methane].[17] However, to take the dinuclear complex $[Pt_2(terpy)_2L]^{3+}$ as a model for solid $[Pt(terpy)Cl][CF_3SO_3]$ needs caution as the former system has shorter Pt···Pt separations of 3.090(1) and 3.071(1) Å. Nevertheless, a weak interaction between two $[Pt(terpy)Cl]^+$ cations is anticipated in the solid state. According to previous studies,[1] such interaction would lead to a red shift in the absorption spectrum from the monomer to the dimer and thus

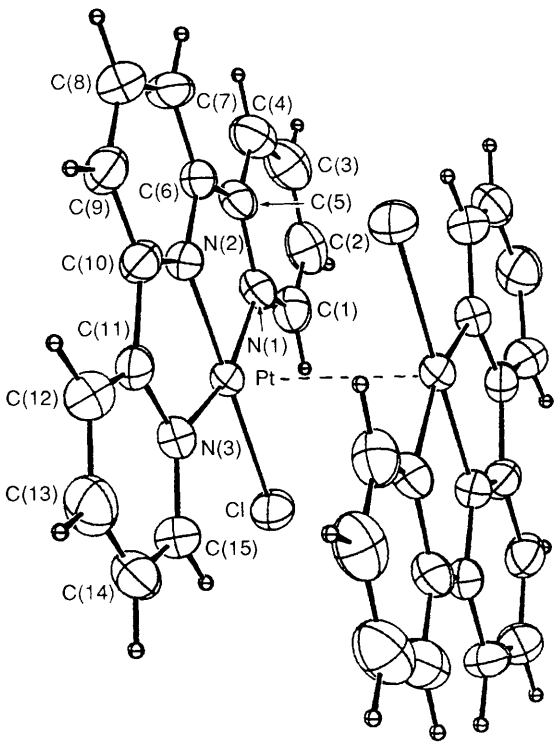

Fig. 6 A perspective drawing of the $[Pt(terpy)Cl]^+$ cation

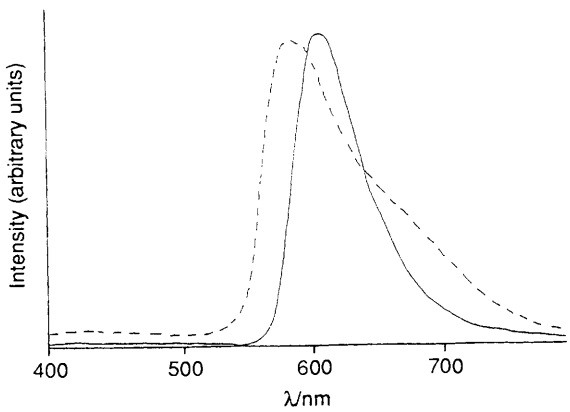

Fig. 7 Room temperature (– – –) and 77 K (———) emission spectra of a microcrystalline sample of $[Pt(terpy)Cl][CF_3SO_3]$

the orange-red colour of solid $[Pt(terpy)Cl][CF_3SO_3]$ is due to the $d_{\sigma^*} \longrightarrow \pi^b$ transition (see Fig. 1).

Fig. 7 displays the emission spectra of a microcrystalline sample of $[Pt(terpy)Cl][CF_3SO_3]$ at room temperature and at 77 K. In contrast to its emission in butyronitrile glass (Fig. 4), the solid-state emission is considerably lower in energy and structureless. The room-temperature spectrum is composed of an asymmetric band centred at 600 nm with a shoulder at ≈ 700 nm. At 77 K the band width is reduced and the emission energy (λ_{max}) shifts from 600 to 625 nm. Since $[Pt(terpy)Cl]^+$ exists as a monomer in glass solution, the difference between Figs. 4 and 7 has to be related to the weak interaction between two $[Pt(terpy)Cl]^+$ units in the solid state, as described earlier.

As described later, the spectrum in Fig. 7 is similar to the emission spectrum of $[Pt_2(terpy)_2L]^{3+}$ (Fig. 8). We assign the red emission of solid $[Pt(terpy)Cl][CF_3SO_3]$ to the $(\pi^b \longrightarrow d_{\sigma^*})$ transition (see Fig. 1). The same assignment has been made by Miskowski and Houlding[1b] to account for the emission of stacked $[Pt(bipy)(CN)_2]$ and double salts such as $[Pt(bipy)_2][PtCl_4]$.

Spectroscopic Properties of $[Pt_2(terpy)_2L]^{3+}$.—The spectroscopic properties of $[Pt_2(terpy)_2L]^{3+}$ have been communicated previously.[2] Its absorption spectrum (Fig. 8) features a low-energy absorption band at 483 nm (ε_{max} = 2.7 × 10^3 dm^3 mol^{-1} cm^{-1}), which has been assigned to the spin-allowed $d_{\sigma^*} \longrightarrow \pi^b$ transition.

Upon excitation of the complex at 483 nm a red emission was observed. When the emission spectrum of a microcrystalline sample of $[Pt_2(terpy)_2L][ClO_4]_3$ was recorded at 77 K (Fig. 8) the bandwidth was reduced and the band became asymmetric. However, the emission maximum is close to that measured in acetonitrile at room temperature (λ_{max} = 620 nm).[2] Fig. 9 shows the emission spectrum of $[Pt_2(terpy)_2L][ClO_4]_3$ measured in a MeOH–EtOH (1:4 v/v) glass at 77 K. Two emissions, (*i*) a vibronically structured band around 470–600 nm and (*ii*) a structureless broad band centred at ≈670 nm, are found. The vibronic spacings between the 0–0 and 0–1

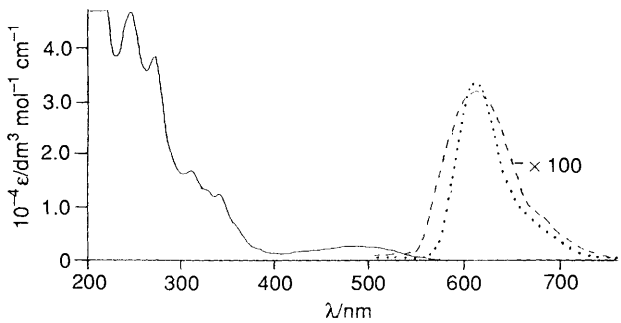

Fig. 8 Room-temperature absorption (MeCN) (———) and emission spectra (– – –, degassed MeCN solution, room temperature; ···, microcrystalline sample, 77 K) of $[Pt_2(terpy)_2L][ClO_4]_3$

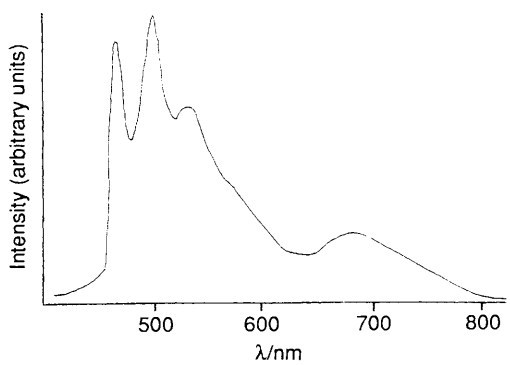

Fig. 9 Emission spectrum of a MeOH–EtOH (1:4 v/v) glass solution of $[Pt_2(terpy)_2L][ClO_4]_3$ at 77 K

transitions of the high-energy emission are about 1450 cm^{-1}, which compare favourably with the ground-state vibrational frequency of terpy. The Huang–Rhys factors found in frozen dimethylformamide, butyronitrile and MeOH–EtOH glass spectra are 1.1, 1.9 and 1.1 respectively. We suggest that the emission at 470–600 nm is intraligand in origin. The structureless broad emission band at 670 nm is assigned to the $^3(d_{\sigma^*}\pi^b)$ state.

While dual emissions were observed in the glass and frozen solutions, only the $^3(d_{\sigma^*}\pi^b)$ emission was found in the solid state and in fluid solution. The equilibrium geometries of the $^3(\pi\pi^*)$ and $^3(d_{\sigma^*}\pi^b)$ states are expected to be different. Thus internal conversion between these two states must involve molecular distortion. A rigid-matrix glassy or frozen solution would render the molecular distortion less favourable and this accounts for the observation of dual emissions. Dual emissions from the $^3(\pi\pi^*)$ and ^{3}m.l.c.t. excited states had previously been reported in $[Cu(phen)(PPh_3)_2]^+$.[18]

Vogler[1d] and Che[1c] and co-workers have independently reported the excimer formation between the ground and excited states of Pt(α-diimine)$(CN)_2$ complexes in solution: $Pt \xrightarrow{h\nu} Pt^* + Pt \xrightarrow{k_f} Pt_2^* \xrightarrow{k_r} Pt + Pt$. Kunkley and Vogler[1d] suggested that the excimeric interaction involves the formation of a metal–metal bond, whereas a mixture of Pt d_{z^2}–d_{z^2} and ligand π–π interaction was suggested by Che and co-workers.[1c] On the other hand, Miskowski and Houlding[1a] introduced organic-like π–π excimeric interaction to account for the red shift and structureless solid-state emission of $[Pt(bipy)_2]^{2+}$ and $[Pt(phen)_2]^{2+}$. Considering two interacting platinum polypyridyl units, the excited state of $[Pt_2(terpy)_2L]^{3+}$ may act as an 'electronic analogue' of the excimers.

Conclusion

This work has demonstrated that $[Pt_2(terpy)_2L]^{3+}$ and $[Pt(4'R\text{-}terpy)Cl]^+$ are new classes of d^8 metal complexes which exhibit emission in fluid solution at room temperature. One remarkable feature is that the photophysical properties of $[Pt(terpy)L']^{n+}$ and $[Pt(4'R\text{-}terpy)Cl]^+$ are sensitive to the auxiliary ligand L′ and substitution on the terpy ligand. This provides a means to tune the excited-state properties of the complexes. Using different substituted terpyridine and L′, the emissive state changes from ^{3}i.l. to ^{3}m.l.c.t. Preliminary electrochemical and spectroscopic studies revealed that $[Pt(4'R\text{-}terpy)Cl]^+$ are powerful photooxidants with $E°(Pt^{II})^* + e^- \longrightarrow Pt^I$ ranging from 0.85 to 0.93 V *vs.* Ag–$AgNO_3$ depending on the substituent on the phenyl ring of 4R′.[19] It is anticipated that the photochemistry of platinum(II) polypyridyl complexes having long-lived emissive excited states should be as rich as that of the $[Ru(bipy)_3]^{2+}$ system.

Acknowledgements

We acknowledge support from the Hong Kong Research Grant Council, The University of Hong Kong and the Croucher Foundation.

References

1 (*a*) V. M. Miskowski and V. H. Houlding, *Inorg. Chem.*, 1989, **28**, 1529; (*b*) V. M. Miskowski and V. H. Houlding, *Inorg. Chem.*, 1991, **30**, 4446; (*c*) K. T. Wan, C.-M. Che and K.-C. Cho, *J. Chem. Soc., Dalton Trans.*, 1991, 1077; (*d*) H. Kunkely and A. Vogler, *J. Am. Chem. Soc.*, 1990, **112**, 5625; (*e*) C.-M. Che, L.-Y. He, C.-K. Poon and T. C. W. Mak, *Inorg. Chem.*, 1989, **28**, 3081; (*f*) V. H. Houlding and V. M. Miskowski, *Coord. Chem. Rev.*, 1991, **111**, 145; (*g*) J. Biedermann, G. Gliemann, U. Klement, K.-J. Range and M. Zabel, *Inorg. Chim. Acta*, 1990, **169**, 63; (*h*) J. Biedermann, G. Gliemann, U. Klement, K.-J. Range and M. Zabel, *Inorg. Chem.*, 1990, **29**, 1884.
2 H.-K. Yip, C.-M. Che, Z.-Y. Zhou and T. C. W. Mak, *J. Chem. Soc., Chem. Commun.*, 1992, 1369.
3 W. Spahni and G. Calzaferri, *Helv. Chim. Acta*, 1984, **67**, 450.
4 M. Howe-Grant and S. J. Lippard, *Inorg. Synth.*, 1980, **20**, 102.
5 SDP Structure Determination Package, Enraf-Nonius, Delft, 1985.
6 K. W. Jennette, T. J. Gill, J. A. Sadownick and S. J. Lippard, *J. Am. Chem. Soc.*, 1976, **98**, 6159.
7 E.-M. A. Ratilla, B. K. Scott, M. S. Moxness and N. M. Kostić, *Inorg. Chem.*, 1990, **29**, 918; N. M. Kostić, *Comments Inorg. Chem.*, 1988, **8**, 137.
8 J. A. Bailey, V. M. Miskowski and H. B. Gray, *Inorg. Chem.*, 1993, **32**, 369.
9 K. Sone, P. Krumholz and H. Stammreich, *J. Am. Chem. Soc.*, 1955, **77**, 777.
10 R. J. Watt, G. A. Crosby and J. L. Sansregret, *Inorg. Chem.*, 1972, **7**, 1474.
11 M. T. Indelli, C. A. Bignozzi, A. Marioni and F. Scandola, *J. Am. Chem. Soc.*, 1988, **110**, 7381.
12 M. L. Stone and G. A. Crosby, *Chem. Phys. Lett.*, 1981, **79**, 169.
13 C. R. Hecker, A. K. I. Gushurst and D. R. McMillin, *Inorg. Chem.*, 1991, **30**, 538.
14 M. Maestri, C. Deuschel-Cornioley and A. Von Zelewsky, *Coord. Chem. Rev.*, 1991, **111**, 112.
15 C.-M. Che, unpublished work.
16 R. S. Osborn and D. Rogers, *J. Chem. Soc., Dalton Trans.*, 1974, 1002.
17 C.-M. Che, V. W.-W. Yam, W.-T. Wong and T. F. Lai, *Inorg. Chem.*, 1989, **28**, 758.
18 D. J. Casadonte and D. R. McMillin, *J. Am. Chem. Soc.*, 1987, **109**, 331.
19 C.-M. Che, unpublished work.

Received 3rd *June* 1993; *Paper* 3/03158F